Carbohydrate Polymers 156 (2017) 9–18

Contents lists available at ScienceDirect

Carbohydrate Polymers

journal homepage: www.elsevier.com/locate/carbpol

Isolation, purification, characterization and immunostimulatory activity of polysaccharides derived from American ginseng

Xiao-Hong Yu, Ying Liu*, Xian-Ling Wu, Li-Zhai Liu, Wei Fu, Dan-Dan Song

College of Food Engineering, Harbin University of Commerce, Harbin, 150076, China

ARTICLE INFO

Article history:
Received 22 June 2016
Received in revised form 25 August 2016
Accepted 26 August 2016
Available online 28 August 2016

Keywords:
American ginseng
Polysaccharide
Purification
Characterization
Immunostimulatory activity

ABSTRACT

In this study, crude American ginseng polysaccharide (AGPS) was extracted with hot water and preliminarily purified by using resin S-8 and Polyamide columns. Then, it was further purified and separated by DEAE-Sepharose CL-6B and Sepharose CL-6B chromatography, respectively. Five main fractions were obtained, named WPS-1, WPS-2, SPS-1, SPS-2 and SPS-3. Their homogeneities and structural characteristics were elucidated based on UV–vis spectroscopy, High Performance Gel Filtration Chromatography (HPGFC), Gas Chromatography (GC), Scanning Electron Microscopy (SEM), Infrared Spectrum (IR), and NMR Spectroscopy methods. Furthermore, the immunostimulatory effects of these fractions upon splenic lymphocyte proliferation, macrophage phagocytosis and nitric oxide (NO) production, were investigated in vitro. The results indicated that their stimulations could be ordered as SPS-3 > SPS-1 > CPS (crude polysaccharides) > WPS-1 > WPS-2 > SPS-2. Among them, SPS-3 showed more potent immunomodulatory activity and could be explored as a potential immunopotentiating agent for use in functional food or medicine.

1. Introduction

America ginseng (*Panax quinquefolius* L.), a member of the genus *Panax* of the Araliaceae family, originated in Quebec, Canada and Wisconsin, the United States. In the 1980s, *P. quinquefolius* was successfully introduced in China and is now grown widely in many areas, such as Liaoning Province, Heilongjiang Province and the Changbai Mountains in Jilin Province (Ma et al., 1998). Asian ginseng (*Panax ginseng* C.A. Meyer, Araliaceae), which is an ancient Chinese medicine, is well known and is one of the most popular energy boosters today (Li, Cai et al., 2012). Studies have shown that *P. quinquefolius* has positive effects on the cardiovascular, immune and endocrine systems due to its wide range of biological activities and unique pharmacological effects (Assinewe, Arnason, Aubry, Mullin, & Lemaire, 2002; Lemmon, Sham, Chau, & Madrenas, 2012).

Polysaccharides (Ps), one of the main classes of bioactive substances in fungi, algae and higher plants, have been shown to exhibit a wide range of pharmacological activities, including broad immunomodulatory and anti-tumor activities (Kouakou et al., 2013). Similar to Asian ginseng, American ginseng is a multi-use herb containing bioactive compounds such as ginsenosides and polysaccharides. Extensive detailed studies of the ginsenosides derived from this herb have been performed. However, relatively few studies of practical purification methods for *P. quinquefolius* polysaccharides and their structural characteristics and biological activities have been conducted. Until now, only 11 polysaccharides derived from American ginseng roots have been identified (Wang, Yao, Sang, Yang, & Ren, 2015). In recent studies, Wang, Yao et al. (2015), Wang, Huang, Sun, and Pan (2015) and Wilson et al. (2013) demonstrated the immunomodulatory and anti-inflammatory activities of an aqueous polysaccharide extract of American ginseng, which stimulated splenocyte proliferation, enhanced macrophage phagocytosis and promoted cytokine secretion, but the potential active component(s) has/have not been identified. Moreover, little is known about the in vitro immunomodulatory properties of different purified polysaccharide fractions, particularly regarding their physicochemical properties and potential structure-function relationships. Therefore, in this study, the CPS of American ginseng roots was extracted using hot water, purified using effective techniques and fractionated using DEAE Sepharose CL-6B anion-exchange chromatography and Sepharose CL-6B gel chromatography. The physiochemical characteristics, such as the molecular weight, monosaccharide composition, and FT-IR and NMR spectra-based structural features

* Corresponding author at: College of Food Engineering, Harbin University of Commerce,138 Tongda Street, Daoli District, Harbin, Heilongjiang Province 150076, China.

E-mail addresses: yuxiaohong1017@163.com (X.-H. Yu), liuying10420@163.com (Y. Liu), yxf930213@163.com (X.-L. Wu), 13361061037@163.com (L.-Z. Liu), fuwei880303@163.com (W. Fu), sdd901017@163.com (D.-D. Song).

http://dx.doi.org/10.1016/j.carbpol.2016.08.092
0144-8617/

of the major purified fractions were determined. Furthermore, we evaluated the effects of these major fractions on splenic lymphocyte proliferation and macrophage phagocytosis in vitro.

2. Materials and methods

2.1. Materials and reagents

Roots were collected from American ginseng plants that were cultivated for 4 years in the Changbai Mountains of Jilin Province, China. The dried roots were crushed into a fine powder using a pulverizer, and the powder was passed through a 60-mesh screen. The powders were stored in a freezer for later use. Sepharose CL-6B and DEAE Sepharose CL-6B were purchased from Pharmacia Fine Chemical AB (Uppsala, Sweden). The monosacharide standards, glucose (Glc), galactose (Gal), rhamnose (Rha), arabinose (Ara), xylose (Xyl), mannose (Man), glucuronic acid (GlcA) and galacturonic acid (GalA) at >98% purity, ferrozine, trichloroacetic acid (TCA), and the dextran M_w standards (T-50, T-100, T-500, T-1000, T-2000) were all purchased from Sigma-Aldrich (Shanghai, China). Trifluoroacetic acid (TFA), concanavalin A (ConA), papain, 3-(4,5-dimethylthiazol-2-yl)-2, 5-diphenyltetrazoliumbromide (MTT), and lipopolysaccharide (LPS) were purchased from Sigma-Aldrich (St. Louis, MO, USA). Dimethyl sulfoxide (DMSO), RPMI-1640 medium, and fetal bovine serum (FBS) were obtained from Gibco (Grand Island, NY, USA). All the reagents used in this study were of the highest quality available from commercial vendors and were of analytical grade (Wang, Yao et al., 2015; Wang, Huang et al., 2015; Wilson et al., 2013).

2.2. Extraction of crude polysaccharides

The dried roots of *P. ginseng* were extracted using 95% ethylalcohol at 90 °C for 4 h under reflux to remove the alcohol-soluble impurities, such as the ginsenosides, lipids and pigments. The supernatant was removed, and the residue was then extracted three times using distilled boiling water at a ratio of 25:1 (w/w) for 3 h. After centrifugation, (4000 rpm for 10 min, at 20 °C), the supernatant was concentrated in a rotary evaporator under reduced pressure, and then a four-fold volume of ethanol was added to the concentrate to precipitate the polysaccharides overnight at 4 °C. The precipitate was collected and was washed with absolute ethanol, acetone and ether, in this order. The residue was lyophilized and was stored in a desiccator at room temperature for later use.

2.3. Isolation and purification of the crude polysaccharides

Prior to purification, the crude American ginseng polysaccharide (AGPS) contained many impurities, mainly proteins and pigments. To determine an effective method for deproteinization of the crude AGPS, the four following methods were compared: Sevag, trichloroacetic acid (TCA), papain, and polyamide method. To determine an effective method for decolorization, the three following methods were compared: activated carbon adsorption, hydrogen peroxide (H_2O_2) treatment and macroporous resin S-8 adsorption. These methods for crude polysaccharide purification were performed as described by Yang, Meng et al. (2012), Yang, Pei et al. (2012). Ten grams of dried crude polysaccharides was redissolved in 1000 mL of distilled water to produce a 10 mg/mL solution. A 50-mL sample of this solution was treated using each deproteinization and decolorization method. The treatments were performed in parallel. One sample group was treated five times using the Sevag method, one sample group was treated with 5% TCA, one sample group was treated with 0.5% papain, and one sample group was treated with 1.5% powdered activated carbon. Polyamide (20 g) and macroporous resin S-8 (35 g) were packed into two columns (Φ16 mm × 300 mm) for deproteinizing and decolorizing using the dynamic adsorption test, according to the method of Jiang, Sun, He, and Shao (2012). The polysaccharide and protein contents were determined using the phenol-sulfuric acid method and the Bradford method, respectively. The pigment content was determined by colorimetry at 400 nm, which was the maximum pigment absorption wavelength determined using whole-wave length scanning. The crude and post-purified polysaccharide solutions were both evaluated using a visible-light spectrophotometer. The rates of deproteinization (DPR), decolorization (DCR) and polysaccharide loss (PSLR) were calculated using the following previous applied equations (Zhang, Du, Zhou, Jie, & Hui, 2011):

$$DPR = [preOD_{595}\text{-postOD}_{595}/\text{preOD}_{595}] \times 100\%$$

$$DCR = [preOD_{400}\text{-postOD}_{400}/\text{preOD}_{400}] \times 100\%$$

$$PSLR = [preOD_{490}\text{-postOD}_{490}/\text{preOD}_{490}] \times 100\%$$

A 400-mg sample of preliminarily purified polysaccharides was redissolved in 20 mL of distilled water and was centrifuged at 4000 rpm for 15 min. The polysaccharides in the supernatant were further purified and isolated using size-exclusion and anion-exchange chromatography. First, a DEAE Sepharose CL-6B column (Φ26 mm × 300 mm) was equilibrated with distilled water, and then was eluted successively using distilled water and NaCl solutions of increasing ionic strength (0.1, 0.2, 0.3, 0.4, 0.5 and 2.0 M) at a flow rate of 5 mL/min. The eluants were collected at 5 mL/tube and then were combined and concentrated to obtain the main fractions, which were further fractionated using size-exclusion chromatography on a Sepharose CL-6B column (Φ26 mm × 600 mm) that was eluted using 0.1 M NaCl at a flow rate of mL/min. The eluant was collected at 2 mL/tube of eluant. The total carbohydrate content of the eluant in each tube was monitored using the phenol-sulfuric acid method. The uronic acid content was determined using a modified hydroxydiphenyl assay, using GlcA as the standard. The main fractions were collected, dialyzed and lyophilized to obtain the purified fractions that were evaluated for immunostimulatory activity.

2.4. Characterization of the purified fractions

2.4.1. Determination of the homogeneity and molecular weight of polysaccharide fractions

Five milligrams of the purified polysaccharides were dissolved in 5 mL of distilled water. The homogeneity and molecular weight distribution of the polysaccharides were determined using spectroscopy and high-performance gel filtration chromatography (HPGFC), respectively. A 20 μL sample was injected into the HPGFC column and the column was eluted with distilled water at a flow rate of 0.5 mL/min (40 °C, 1.6 MPa). The peaks were detected using a SHIMADZU CLSS-VP system equipped with an ULtrahydrogel™ linear column (7.8 mm × 300 mm) and a refractive index detector (RID-10A). The average M_w (weight-average molecular weight) values of the polysaccharides were determined using a standard curve produced using dextran T standards of known M_W (T-50, T-100, T-500, T-1000, T-2000). The standard curve-based equation used for calculating the average M_w values was as follows:

$$\lg M_w = -3.9042(\text{Kav}) + 7.5638; R^2 = 0.9686$$

where Kav was the effective distribution coefficient.

2.4.2. Scanning electron microscopy (SEM)

SEM was used to characterize the micro-structures and surface morphologies of the materials in the fractions. Dried samples of the five purified fractions were fixed on a silicon wafer, coated using ion

beam sputtering deposition, and then examined at a 10 KV acceleration voltage in a vacuum specimen chamber. The shape and surface characteristics were observed and images were collected using a scanning electron microscope (SEM, S-4800, Hitachi, Japan), followed by magnification at 100–10,000×.

2.4.3. Monosaccharide composition analysis

Each fraction (10 mg) was hydrolyzed using TFA (2 M, 1 mL) at 110 °C for 4 h in an oven. Subsequently, the acid was completely removed by flash evaporation in a water bath temperature at 50 °C and the residue was co-distilled three times using methanol. The hydrolyzed samples and the monosaccharide alditol acetates were prepared following the methods of Sudhamani, Tharanathan, and Prasad (2004) and Yang, Meng et al. (2012), Yang, Pei et al. (2012). The samples (0.1 μL) were injected into an Agilent 6890 N GC system (AgilentTechnologies, Wilmington, USA) equipped with an HP-5 fused silica capillary column (30 m × 0.32 mm × 0.25 mm) and a flame ionization detector (FID). The column temperature was programmed to increase from 140 °C (maintained for 2 min) to 170 °C at a rate of 7 °C/min and then to increase to 260 °C at a rate of 3 °C/min. The injection temperature was 280 °C, the detector temperature was 300 °C, and the flow rate of the N_2 carrier gas was 1.0 mL/min.

2.4.4. IR spectroscopic analysis

IR spectra were recorded using the KBr-disk method using a Nicolet Fourier transform infrared (FTIR) spectrometer (Nicolet Nexus 470, Thermo Nicolet Co., Madison, WI, USA). The samples were ground with spectroscopic grade potassium bromide (KBr) and then were pressed into a 1 mm pellet for IR analysis at a frequency range of 4000–400 cm^{-1} and a resolution of 4 cm^{-1}.

2.4.5. NMR analysis

The freeze-dried polysaccharides were treated three times with deuterium oxide and were then dissolved in D_2O (0.5 mL). ^1H and ^{13}C NMR spectra were recorded using a Bruker AM 400 MHz spectrometer (Bruker, Rheinstetten, Germany) at 30 °C. Data processing was performed using standard Bruker XWIN-NMR software.

2.5. Measurement of the immunostimulatory activity

2.5.1. Animals

Specific pathogen-free Jilin mice (male, 8 weeks old, certificate number: SCXK-Ji 2011-004) were provided by the Norman Bethune Health Science Center of Jilin University, China. They were acclimatized for one week before the experiment was conducted. The mice were housed in a rodent facility at 22 ± 1 °C with a 12/12 h light/dark cycle and were supplied with a standard laboratory rodent diet (Laboratory Animal Center of Norman Bethune Health Science, China) and tap water ad libitum. The use of the mice in this experiment followed the guidelines set forth in the U.K. Animals (Scientific Procedures) Act of 1986.

2.5.2. In vitro T-lymphocytes and B-lymphocytes proliferation assays

The splenic lymphocyte proliferation assay was performed as described by Yi et al. (2012) and Sun et al. (2012). Mice were killed by cervical dislocation and their spleens were removed aseptically and then were minced in aseptic phosphate-buffered saline (PBS). The splenocytes were harvested by passing the minced tissues through sterilized meshes (200 mesh) at room temperature. The splenocytes were washed three times using D-Hank's solution and were re-suspended in RPMI 1640 complete medium (Gibco). The splenocytes (100 μL/well, 5×10^6/mL) were seeded in 96-well plates in the presence of concanavalin A (ConA) (0.005 mg/mL) or lipopolysaccharide (LPS) (0.01 mg/mL). Filter-sterilized samples of the five purified polysaccharide fractions (final concentrations of 50, 100, 200, 300 and 400 μg/mL) were added to the wells. The plates were incubated at 37 °C in a 5% CO_2 incubator for 68 h. Next, a 5 mg/mL MTT (3-[4,5-dimethylthiazol-2-yl] -2, 5-diphenyltetrazolium bromide, Sigma) solution was added to each well and the plates were incubated for another 4 h. Then, 100 μL/well of acidified isopropyl alcohol was added, and the plate was maintained for 12 h to allow the formazan crystals to dissolve. The absorbance at 570 nm was measured using a Bio-Rad microplate reader (Hercules, CA, USA) (Hwang et al., 2011).

2.5.3. In vitro macrophage phagocytosis assay

The macrophage phagocytosis assay was performed as described by Sun et al. (2012). Macrophages were obtained from normal mice by peritoneal lavage using D-Hank's solution. After centrifugation, the cells were re-suspended in RPMI 1640 complete medium. The cells were placed in a flat-bottomed culture plate and were incubated at 37 °C for 4 h in a 5% CO_2 incubator. The medium was removed and the non-adherent cells were washed out, after which the mono-layered macrophages were collected. Phagocytosis by the macrophages was evaluated using the neutral red uptake method.

In brief, the macrophages were seeded in 96-well plates at a density of 2×10^5 cells/well.The cells were incubated in only the medium or in medium containing samples of each fraction at various final concentrations (50, 100, 150 and 200 μg/mL). LPS (10 μg/mL) was used as the positive control. After 24 h of incubation in a 5% CO_2 incubator, the media were discarded and a 0.075% neutral red dye solution was added to each well (100 μL/well). The plate was incubated for another 3 h and then was washed three times using PBS (pH 7.2). Finally, 100 μL of cell lysate (0.1 mol/L acetic acid/ethanol 1:1) was added to each well and the plate was placed in a 5% CO_2 incubator overnight, after which the absorbance at 540 nm was measured using a microplate reader.

2.5.4. In vitro nitric oxide (NO) production assay

NO production was measured as previously described by Gao, Wang, Lien, and Trousdale (1996) and Sun et al. (2012). Briefly, peritoneal macrophages (2.0×10^5 cells/well) were plated in 48-well plates and were treated with polysaccharides for 48 h as described in Section 2.5.3. The media were collected and were mixed with an equal volume of Griess reagent (1% sulfanilamide in dd H_2O, 0.1% *N*(1-naphthyl)ethylenediamide in 5% phosphoric acid). After 10 min, the absorbance at 540 nm was measured using a microplate reader. Sodium nitrite was used to generate a standard curve.

2.5.5. Statistical analysis

The data were expressed as the mean values ± standard deviations. The significance of the differences was evaluated using a one-way analysis of variance (ANOVA) followed by the Student–Newman–Keuls test, using SPSS 11.5 software. A value of $P < 0.05$ was considered to indicate a significant difference.

3. Results

3.1. Polysaccharide extraction, isolation and purification

The yield of the CPS extracted from *P. quinquefolius* was approximately 14.97% and its protein content was 0.36%. The efficacy of the different preliminary purification methods was evaluated according to the rates of decolorization, deproteinization and polysaccharide loss of the resultant preparations (Fig. 1). The results showed that polyamide column chromatography was better than the other deproteinization methods tested. As shown in Fig. 1a, the rates of deproteinization and polysaccharide loss obtained using this method were 95.42% and 10.86%, respectively. The effects of the

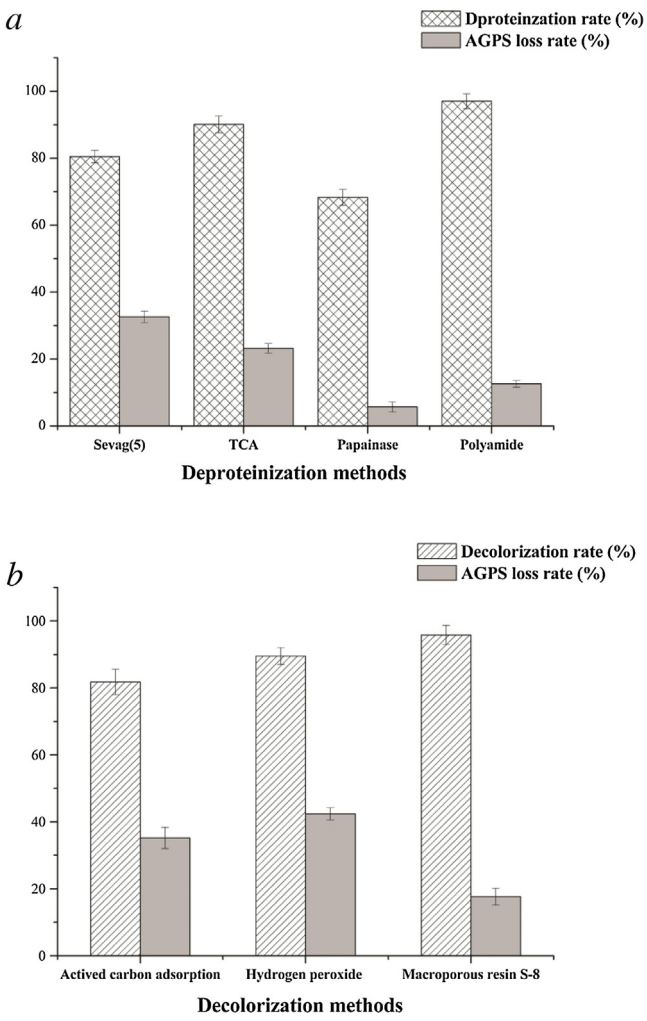

Fig. 1. Comparison of the efficacy of the different preliminary purification methods used to treat the crude polysaccharides. (a) Deproteinization methods, (b) Decolorization methods.

decolorization methods on the crude extract are shown in Fig. 1b. Macroporous resin S-8 treatment provided the highest decolorization rates among the various methods tested; its decolorization rate reached 91.43% and the polysaccharide loss rate was 17.82%.

The preliminarily purified AGPS was fractionated using anion-exchange chromatography. The elution curve had (Fig. 2a) one broad peak of water-eluted polysaccharide (WPS), obtained at a yield of 32.82%, and three peaks of salt-eluted polysaccharide (SPS) obtained at yields of 5.82%, 6.15% and 9.42%, respectively. Each main polysaccharide fraction was further fractionated using size-exclusion chromatography. The WPS was eluted using 0.1 M NaCl to give two single peaks, and the SPS was eluted as three major peaks. Two neutral polysaccharides and three acidic polysaccharides were obtained (named WPS-1, WPS-2, SPS-1, SPS-2 and SPS-3) and were selected for analysis based on their total carbohydrate elution profiles (Fig. 2b).

3.2. Characterization of the polysaccharide fractions

3.2.1. Physicochemical properties and monosaccharide composition

The homogeneity and M_w of the components in the five fractions were determined using UV–vis spectroscopy and HPGFC, respectively. Analysis of the UV–vis spectrum (190–600 nm) of each fraction showed that there was no absorption in the range of 260–280 nm, which indicated that none of the five polysaccharide fractions contained nucleic acids or proteins. The HPGFC profiles showed that each polysaccharide was represented by a single and symmetrically sharp peak, revealing that the content of each was a homogeneous polysaccharide. The physicochemical properties and monosaccharide compositions of these polysaccharides are summarized in Table 1.

Scanning electron microscopy (SEM) (500×) (Fig. 3) showed that the contents of the neutral WPS-1 fraction had a fragmented and honeycomb-like morphology. The WPS-2 contents resembled large, hollow rugby balls interspersed with fragmented structures. SPS-1 contained irregular structures and fibrous filaments and ribbons with branches. SPS-2 also contained irregular structures and fibrous filaments and ribbons with branches. SPS-3 contained structures resembling withered leaves and lamelliform and random coil-shaped structures. The morphologies and textures of the structures were also observed under high magnification (10,000×). Smooth, compact structures were observed in WPS-1 (Fig. 3a), SPS-2 (Fig. 3d) and SPS-3 (Fig. 3e). Rough and dispersed structures were observed in WPS-2 (Fig. 3b) and SPS-1 (Fig. 3c).

3.2.2. IR spectroscopic analysis

As shown in Fig. 4, the FT-IR spectra of the purified WPS-1, WPS-2, SPS-1, SPS-2 and SPS-3 fractions displayed absorption peaks typical of polysaccharides in the range of 4000–400 cm^{-1} (Chokboribal et al., 2015). The broadly stretched intense band at 3420 cm^{-1} was due to the stretch vibration of the O—H bond. The signal at 2925 cm^{-1} can be attributed to the stretch vibration of the C—H bond of CH_3 or CH_2. The relatively strong absorption peak at approximately 1650–1540 cm^{-1} indicated the characteristic stretching vibration of the C=O bond. The band at 1420 cm^{-1} was assigned to the bending vibration of the C—H bond. The absorbance of the polysaccharides in the range of 1160–1020 cm^{-1} are due to their C—O—C and C—O—H linkages (Shang et al., 2012).

3.2.3. NMR analysis

The 400-MHz ^1H and ^{13}C NMR spectra of each fraction are shown in Fig. 5. NMR spectroscopic analysis demonstrated that all of the fractions contained heteropolysaccharides. The ^1H signal at 4.70 ppm is due to D_2H. The chemical shifts from 3.5 to 4.5 ppm were assigned to the protons of carbons C-2 to C-6 of the glycocidic ring. ^1H signals appeared in the anomeric region of 5.12–5.44 ppm, which indicated that the WPS-1 and WPS-2 heteropolysaccharides existed mostly in the α-type configuration (Fig. 5A). The resonance signals of anomeric H-1 at 4.88–5.30 ppm in the ^1H NMR spectra of SPS-1 and SPS-3 confirmed the presence of both α-type and β-type glycosidic bonds (Fig. 5A). In the ^{13}C NMR anomeric region, the signals at 107.3–109.3 ppm were assigned to Araf, whereas the signals at 102.9–104.2 ppm were assigned to Galp and Glcp (Fig. 5B). The ^{13}C signal at 67–70 ppm confirmed the presence of (1 → 6) glycosidic linkages, whereas that at 80–83 ppm implied the presence of (1 → 3/4) glycosidic linkages. Due to the poor water solubility of SPS-2, the ^1H and ^{13}C signals were weak and were therefore difficult to analyze.

3.3. Immunostimulatory activities of the polysaccharide fractions

3.3.1. Effects on splenic lymphocyte proliferation

The immunological activities of the purified polysaccharide fractions were investigated by testing their effects on lymphocyte proliferation in vitro. The effects of these fractions on normal (without mitogen) and mitogen-induced splenic lymphocyte proliferation were investigated in the dose range of 50–400 μg/mL, as shown in Table 2. There were no significant differences in the effects of the fractions on normal proliferation at 50–400 μg/mL ($P > 0.05$), and all of the fractions strongly promoted mitogen-

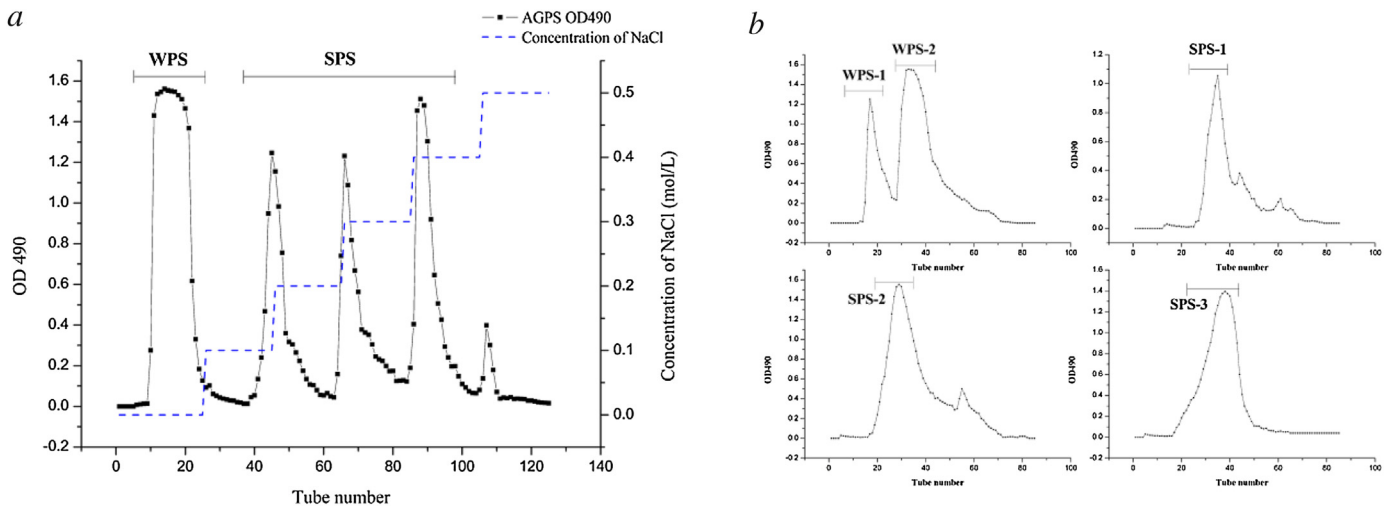

Fig. 2. Stepwise elution curve of the AGPS fractionated using DEAE Sepharose CL-6B chromatography (a) and elution curves subsequently obtained using Sepharose CL-6B chromatography (b).

Table 1
Physicochemical properties of the polysaccharides isolated from American ginseng.

Fraction	Sugar content (%)	Protein content (%)	Uronic acid content (%)	Molecular weight (Da)	Solubility	Sugar component (mol%)							
						Ara	Rha	Xyl	Man	Gal	Glc	GalA	GlcA
AGPS	81.73	0.36	15.43		++								
WPS-1	98.79	0	0	1.54×10^6	+++	21.2	2.3	–	2.6	18.7	55.2	–	–
WPS-2	99.54	0	0	1.41×10^4	++++	27.9	1.7	–	2.9	20.7	46.8	–	–
SPS-1	99.42	0	20.13	3.62×10^5	++++	22.3	–	6.9	9.2	28.6	15.9	13.6	3.5
SPS-2	98.05	0	25.78	9.70×10^6	+	14.2	–	5.3	7.9	22.5	25.3	16.9	7.9
SPS-3	99.38	0	31.83	5.12×10^5	++++	19.2	2.1	9.6	12.0	15.2	11.5	26.3	4.1

The data are presented as mol% of each sugar. Individual components were identified and quantified using GC. +, degree of water solubility, – not detected.

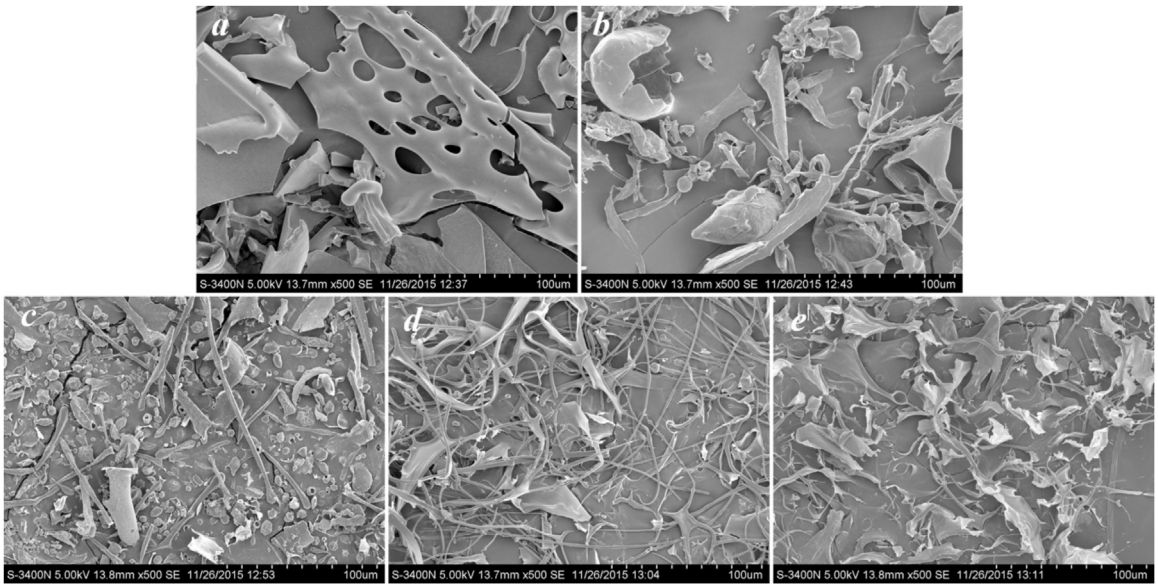

Fig. 3. Scanning electron micrographs (500×) of WPS-1(a), WPS-2(b), SPS-1(c), SPS-2(d) and SPS-3(e).

induced proliferation at 200–300 μg/mL ($P < 0.05$ or $P < 0.01$). In the case of ConA-induced proliferation, WPS-1, WPS-2, and SPS-1 significantly stimulated lymphocyte proliferation at 300 μg/mL ($P < 0.01$) and suppressed it at 400 μg/mL ($P < 0.05$) compared with the ConA control. In the case of LPS-induced proliferation, WPS-1, WPS-2, SPS-1 and SPS-3 significantly increased the proliferation rate at 200–400 μg/mL ($P < 0.05$ or $P < 0.01$, in direct correlation with the dose) compared with the LPS control. Among the fractions, SPS-3 exerted strong dose-dependent immunostimulatory activity on both ConA- and LPS-induced proliferation at 200–400 μg/mL ($P < 0.01$).

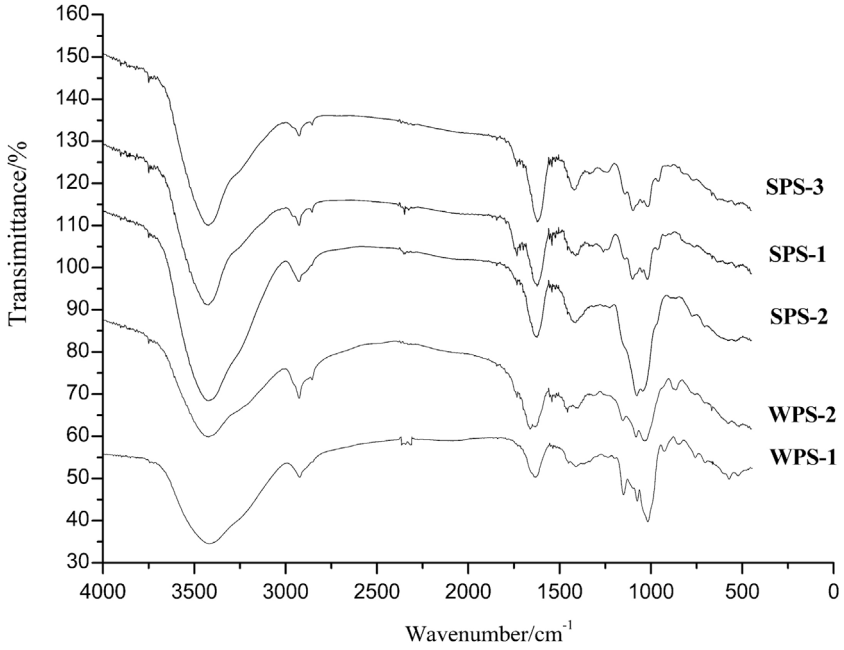

Fig. 4. IR spectra of each fraction obtained from American ginseng.

Table 2
Effects of the five fractions on splenic lymphocyte proliferation.

Dose (μg/mL)	Mitogen	WPS-1	WPS-2	SPS-1	SPS-2	SPS-3
0	–	0.563 ± 0.028	0.582 ± 0.007	0.571 ± 0.005	0.576 ± 0.017	0.578 ± 0.004
	ConA	0.751 ± 0.004	0.783 ± 0.012	0.729 ± 0.012	0.726 ± 0.003	0.785 ± 0.009
	LPS	0.860 ± 0.013	0.868 ± 0.005	0.851 ± 0.009	0.878 ± 0.004	0.872 ± 0.005
50	–	0.550 ± 0.006	0.572 ± 0.020	0.560 ± 0.004	0.574 ± 0.006	0.565 ± 0.014
	ConA	0.763 ± 0.017	0.775 ± 0.011	0.724 ± 0.008	0.746 ± 0.013	0.768 ± 0.023
	LPS	0.869 ± 0.009	0.864 ± 0.007	0.873 ± 0.013	0.865 ± 0.037	0.881 ± 0.009
100	–	0.581 ± 0.006	0.579 ± 0.017	0.575 ± 0.012	0.580 ± 0.007	0.585 ± 0.019
	ConA	0.774 ± 0.008	0.782 ± 0.007	0.742 ± 0.006	0.776 ± 0.037	0.770 ± 0.004
	LPS	0.872 ± 0.015	0.876 ± 0.015	0.883 ± 0.009	0.879 ± 0.008	0.892 ± 0.010
200	–	0.602 ± 0.012	0.599 ± 0.012	0.610 ± 0.006	0.579 ± 0.017	0.594 ± 0.006
	ConA	0.843 ± 0.005*	0.852 ± 0.008*	0.841 ± 0.010*	0.794 ± 0.006	0.974 ± 0.017**
	LPS	0.959 ± 0.008*	0.960 ± 0.020*	0.958 ± 0.011*	0.948 ± 0.031*	1.175 ± 0.009**
300	–	0.578 ± 0.010	0.582 ± 0.007	0.571 ± 0.012	0.576 ± 0.010	0.575 ± 0.023
	ConA	1.057 ± 0.007**	1.025 ± 0.013**	1.032 ± 0.007**	0.921 ± 0.012*	1.136 ± 0.012**
	LPS	1.203 ± 0.004**	1.232 ± 0.010**	1.241 ± 0.019**	0.966 ± 0.009*	1.231 ± 0.007**
400	–	0.569 ± 0.013	0.582 ± 0.008	0.571 ± 0.006	0.580 ± 0.006	0.575 ± 0.008
	ConA	0.902 ± 0.022*	0.912 ± 0.004*	0.919 ± 0.015*	0.926 ± 0.021*	1.148 ± 0.005**
	LPS	1.184 ± 0.009**	1.237 ± 0.004**	1.245 ± 0.008**	0.943 ± 0.014*	1.314 ± 0.020**

The splenocyte proliferation rate was measured using the MTT method. The proliferation stimulatory activities were expressed as the units of absorption at 570 nm. The data shown are the mean values ± SD (n = 6). *P < 0.05, **P < 0.01 compared to the untreated control.

3.3.2. *Effects on macrophage phagocytosis*

The immunostimulatory effects of the CPS and each purified fraction on the phagocytosis and NO (as nitrite) production of macrophages in vitro were investigated. As shown in Fig. 6a, the fractions had enhanced macrophage phagocytosis to various degree in the dose range of 50–200 μg/mL. WPS-1, WPS-2 and SPS-2 had no significant effects on phagocytic activity in the dose range of 50–200 μg/mL, whereas SPS-3, SPS-1 and CPS enhanced macrophage phagocytosis in a dose-dependent manner compared to the control level. At 200 μg/mL, SPS-3, SPS-1 and CPS significantly increased macrophage phagocytosis to levels of 88.5%, 75.4% and 70.6%, respectively. The extent of stimulation followed the order SPS-3 > SPS-1 > CPS, as shown in Fig. 6a. LPS (lipopolysaccharide) was used as the positive control. The production of NO was assessed using the Griess reaction assay. Fig. 6b shows that SPS-3 strongly stimulated the NO production of murine macrophages in a dose-dependent manner ($p < 0.01$), whereas SPS-2 had no effect on NO production in the range of the tested doses. The amount of NO production stimulated by each fraction followed the order SPS-3 > SPS-1 > CPS > WPS-1 > WPS-2, which was consistent with the levels of phagocytic activity observed upon treatment with these fractions.

4. Discussion

In general, the techniques used to extract, purify and separate plant polysaccharides can affect their potencies and characteristics (Benhabiles, Drouiche, Lounici, Pauss, & Mameri, 2013; Ming et al., 2011; Mu, Zhu, Zhao, Zhou, & Jia, 2009). Polysaccharides extracted from plants generally contain substantial amounts of

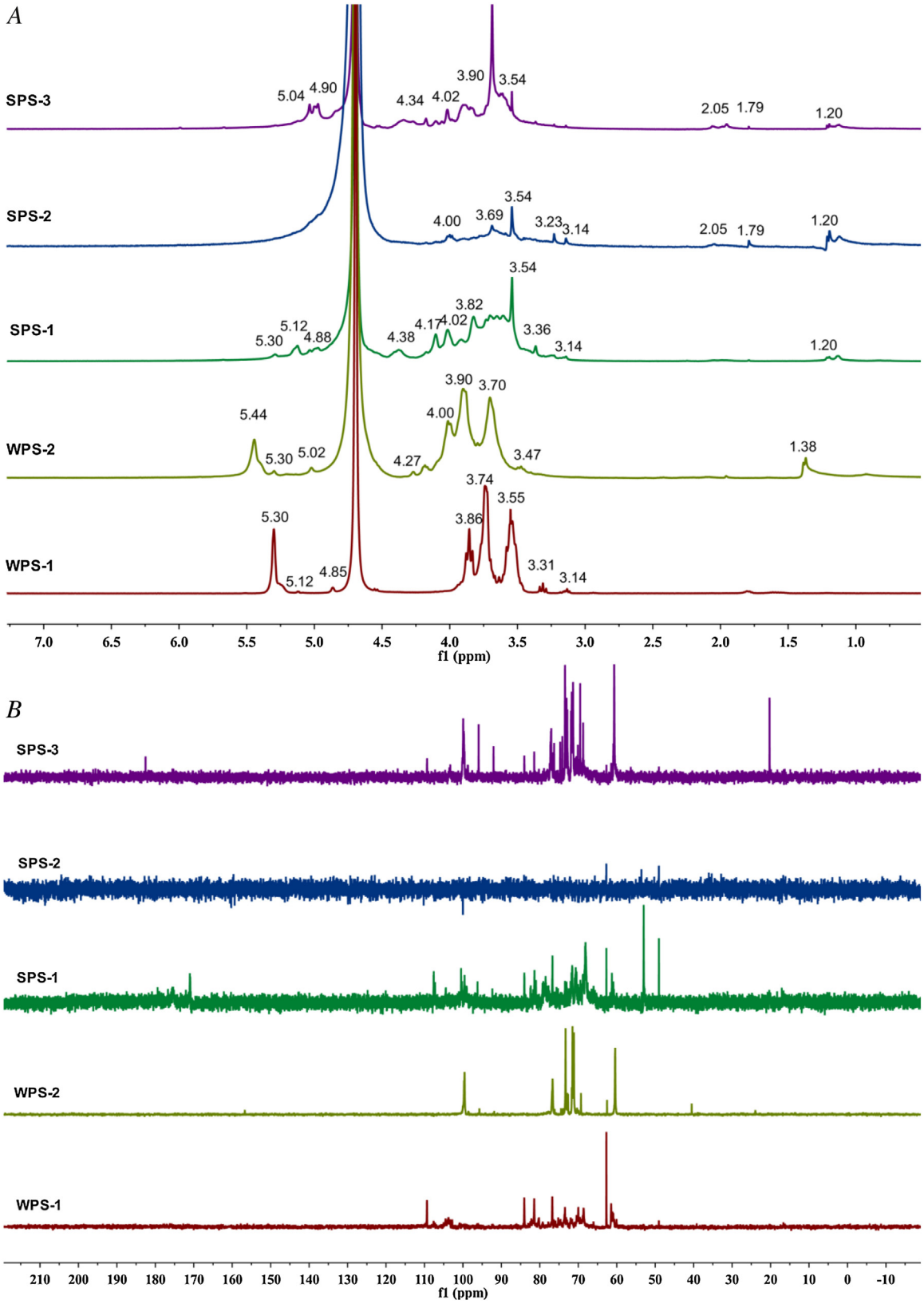

Fig. 5. NMR spectra of each fraction. (A) ^{1}H NMR and (B) ^{13}C NMR spectra.

impurities, particularly pigments and proteins. The presence of impurities greatly affects the subsequent processes of structural characterization and biological activity analysis (Hu, Liang, & Wu, 2015; Liu et al., 2010). Therefore, it was necessary to develop novel methods for decolorizing and deproteinizing the crude polysaccharide extract of American ginseng. Zhang et al. (2011) achieved a deproteinization rate of 85.17% and a polysaccharide loss rate of 28.89% by using a combination of the Sevag and TCA meth-

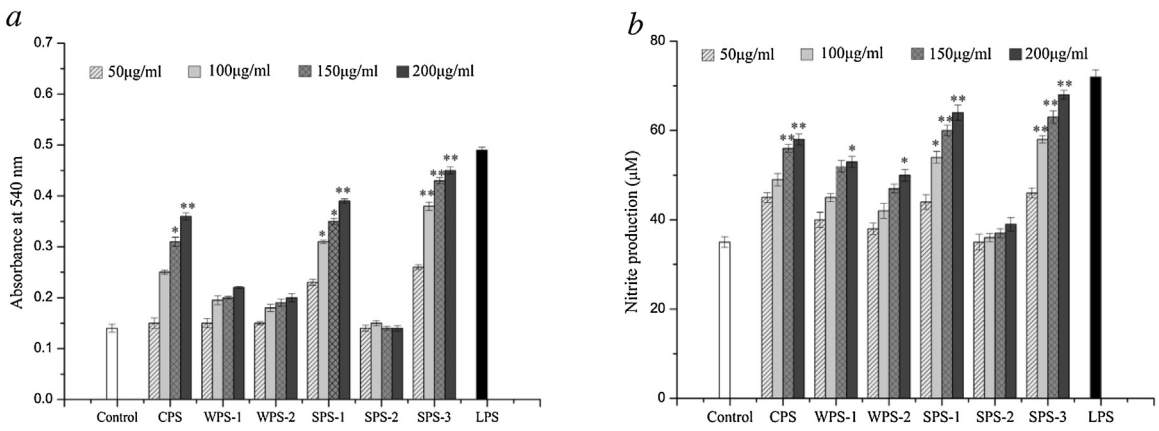

Fig. 6. The immunostimulatory effects of the CPS and each purified fraction on (a) macrophage phagocytosis and (b) NO (as nitrite) production by macrophages in vitro. The culture medium and LPS (10 μg/mL) were used as the blank control and the positive control, respectively. Two independent experiments were performed and the data shown are the mean values ± SD (n = 6). The data sets were evaluated using an ANOVA. *P < 0.05, **P < 0.01 versus negative control group.

ods. In the present study, effective methods for deproteinizing and decolorizing a crude polysaccharide preparation were explored. Fig. 1(a) shows that the deproteinization rates obtained using TCA and polyamide were 91.2% and 94.9%, respectively. However, the TCA deproteinization method is based on acid hydrolysis, which also hydrolyzes glycosidic bonds to a certain extent. The properties and structural features of the AGPS would be destroyed by this chemical reaction. Thus, the polyamide technique is a green method for deproteinizing polysaccharide solutions, and the polysaccharide loss rate obtained using this method was only 10.86%. There were no significant differences in the decolorization rates achieved using the activated charcoal, H_2O_2 or macroporous resin S-8 methods, as shown in Fig. 1(b). H_2O_2 was higher (90.5%) than that obtained using activated charcoal, but decolorization using H_2O_2 results from its strong oxidative activity, which merely turns the pigments into colorless substances and does not remove natural pigments. Likewise, H_2O_2 may oxidize the polysaccharides, leading to a high polysaccharide loss rate. Compared with the chemical deproteinizing and decolorizing methods, the macroporous resin S-8 and polyamide column chromatographic methods have many advantages, such as a moderate mode of action, a low operating cost, reduced solvent consumption, easy regeneration and almost no polysaccharide degradation occurring during the treatment process (Zhang, Zhao, Meng, & Du, 2014). Therefore, preliminary purification using S-8 resin and polyamide columns is a promising strategy for retaining the majority of the extracted polysaccharides without destroying their native structures and activities.

By sequential purification and isolation using DEAE-Sepharose CL-6B and Sepharose CL-6B chromotography, two neutral polysaccharides and three acidic polysaccharides were obtained. Their physicochemical properties, monosaccharide compositions and molecular masses were determined (Table 1), which were different from those reported by Wang, Yao et al. (2015), Wang, Huang et al. (2015) due to the use of different types of ginseng roots and different isolation conditions. The polysaccharides isolated in the present study had different textures and surface properties, as revealed using SEM. This is the first report of the properties of these individual polysaccharides. The five isolated compounds all exhibited the FT-IR bands characteristics of a polysaccharide (Fig. 4). Notably, the bands in the region of 1200–1000 cm^{-1} in the spectra of WPS-1 and WPS-2, which were eluted using distilled water, had three absorption peaks, which could be assigned to the skeletal modes of pyranose rings (Maity et al., 2011; Pan et al., 2012). The bands in the spectra of SPS-1, SPS-2 and SPS-3 at 1733.95 cm^{-1}, 1702.43 cm^{-1} and 1689.23 cm^{-1} were ascribed to the asymmetric and stretching vibrations of a carboxyl group, indicating a trace of uronic acid in these samples. The characteristic absorption bands at approximately 835 cm^{-1} and 890 cm^{-1} suggested that SPS-1, SPS-2 and SPS-3 simultaneously exist in α-and β-configurations. The bands at 854.04 and 833.81 in the spectra of the neutral polysaccharides WPS-1 and WPS-2 suggested that they had an α-configuration (Prozil, Costa, Evtuguin, Cruz Lopes, & Domingues, 2012). The characteristic peak at approximately 835 cm^{-1}in the IR spectrum of each fraction indicated the presence of β-arabinopyranosyl residues (Wang, Yao et al., 2015; Wang, Huang et al., 2015). None of the IR spectra of the polysaccharide fractions showed absorption at 1620 cm^{-1},which is a characteristic of an amino group, indicating the absence of protein, which demonstrated that the preliminary purification procedures were effective.

Furthermore, NMR spectroscopy was used to structurally characterize the polysaccharides. The signals observed in the ^1H and ^{13}C NMR spectra of each fraction were assigned based on component analysis and published values. The similarity in the anomeric region in the range of 3.00–4.00 ppm of the ^1H NMR spectra of the two neutral fractions, WPS-1 and WPS-2, suggested that they possess a similar backbone structure (Fang, Yin, Yuan, & Chen, 2015). The strong ^1H signals at 5.30 and 5.44 ppm represent α-type glycosidic bonds, consistent with the presence of bands at 854.04 and 833.81 cm^{-1} in the FT-IR spectra of WPS-1 and WPS-2. Accordingly, the signals observed at 99.7, 76.8, 73.5, 69.4, 70.3 and 60.4 ppm in the anomeric region of the ^{13}C NMR spectra of both of these fractions could be assigned to C-1, C-2, C-3, C-4, C-5 and C-6 of →6)- α-D-Glcp-(1 → linkages, respectively (Yi et al., 2012). In addition, the ^1H signal at approximately 5.02 ppm and the ^{13}C signal at 103.8 ppm indicated the presence of (1 → 5)- α-L-Araf in these fractions (Wang, Yao et al., 2015; Wang, Huang et al., 2015). The →4,6)- α-D-Glcp-(1 → linkage in SPS-1 and SPS-2 were demonstrated by the signals at 99.5, 76.6, 74.4, 71.5, 69.9 and 62.5 ppm, and the signals observed at 96.0 and 92.2 ppm might also be attributed to their content of α-D-Glcp (Wang, Yao et al., 2015; Wang, Huang et al., 2015). The ^1H peaks at approximately 4.30 ppm and the ^{13}C peaks at approximately 82.4 are due to the presence of β-D-xylose (Kouakou et al., 2013). The signal at 170.9 ppm was attributed to carboxyl groups bound to methyl groups; whereas the signal at 175.8 ppm was due to the ionic carboxyl group (C-6) of uronic acid (Yu et al., 2010). Furthermore, the ^1H signal at approximately 2.0 ppm and the ^{13}C signal signals at 20.1 ppm suggested that SPS-2 and SPS-3 contain *O*-acetyl groups (Li, Xie, Su, Ye, & Jia, 2012). The compounds containing terminal methyl groups showed ^1H signals at 1.20 ppm (Tian, Yin, Zeng, Zhu, & Chen, 2015). The signals observed at 104.6, 84.0, 73.4, 81.4 and 62.6 ppm in the ^{13}C spec-

trum of SPS-3 could be assigned to the C-1, C-2, C-3, C-4, C-5 and C-6 of →4)- α-D-Manp-(1→ (Mondal, Das, Roy, & Islam, 2012). The ^{1}H signals at 4.88 and 4.90 ppm and the ^{13}C signal at 107.3 and 107.6 ppm confirmed the presence of β-D-Galp in SPS-1 and SPS-2. The ^{13}C signals at approximately 99.8 and 82.4 ppm might have originated from the C-1 and C-4 of →4)-β-D-*R*ha-(1→ in WPS-2 and SPS-3 (Zha, Luo, Luo, & Jiang, 2007). To summarize, WPS-1 and WPS-2 consisted mainly of (1 → 6)-α-D-Glcp and (1 → 5)- α-L-Araf, whereas SPS-1, SPS-2 and SPS-3 consisted mainly of (1 → 6)-α-D-Glcp, (1 → 4)-α-D-Manp, (1 → 5)- α-L-Araf, β-D-Galp and β-D-xylose. SPS-2 and SPS-3 contained O-acetyl groups; WPS-1 and SPS-3 contained (1 → 4)- β-D-*R*hap.

Lymphocyte proliferation is a crucial event in the activation cascade of both the cellular and humoral immune responses (Jin et al., 2010). The T-lymphocyte stimulatory activity of the fractions was evaluated using a ConA-induced splenic lymphocyte proliferation assay, whereas the B-lymphocyte stimulatory activity was evaluated using an LPS-induced proliferation assay employing the same cells (Du, Jiang, Wu, Won, & Choung, 2008). The results obtained indicated that the crude AGPS had a significant effect on mitogen-induced proliferation (Du et al., 2008). However, the effects of the individual bioactive polysaccharides in this preparation have rarely been studied. Our study demonstrated that the different polysaccharide fractions had an obvious effect on lymphocyte proliferation in the concentration range of 200–400 μg/mL (Table 2). Specifically, WPS-1, WPS-2, SPS-1 and SPS-3 significantly promoted the proliferation of B cells in a dose-dependent manner and had a strong inhibitory effect on the ConA-induced proliferation of T cells at the concentration of 400 μg/mL. In contrast, SPS-2 did not significantly promote the proliferation of B cells or T cells in this dose range. These results were consistent with the results obtained using a polysaccharide found to be an α-(1 → 6)-D-glucan and with a molecular weight of 17,000 Da that was isolated from the roots of Panax ginseng C. A. Meyer, which stimulated lymphocyte proliferation (Sun et al., 2012). In addition, bioactive polysaccharides composed mainly of galactose, rhamnose and arabinose, with molecular weights ranging from 10,000 to 150,000 Da, have been reported (Lemmon et al., 2012). The estimated molecular weight of the American ginseng immunostimulatory PS found in our study was within this range. Moreover, the effects of polysaccharides on lymphocytes were found to be closely related to their content of branching chains composed mainly of D-mannopyranosyl residues (Wang et al., 2013). Based on analysis of the sugar compositions of the fractions (Table 1), SPS-3 had a much higher mannose content (12.0%) compared with those of WPS-1 (2.6%), WPS-2 (2.9%), SPS-1 (9.2%) and SPS-2 (7.9%). SPS-3 strongly stimulated lymphocyte proliferation, which is consistent with the immunoregulatory activity of a polysaccharide being positively affected by its mannose content (Yu, Jin, Xin, & He, 2009).

Macrophages are pivotal immunocytes for host defense. Stimulating macrophage phagocytosis is an important way to enhance the immune response (Zheng, Wang, & Li, 2015). The effect of each fraction on macrophage phagocytosis was tested using a neutral red phagocytosis assay, using LPS as the positive control. WPS-1, WPS-2 and SPS-2 were not effective in stimulating macrophage phagocytosis in the range of test doses, whereas CPS, SPS-1 and SPS-3 enhanced macrophage phagocytosis in a dose-dependent manner compared with the control. At 100 μg/mL, SPS-3 significantly increased macrophage phagocytosis, raising the level to 74.3% (Fig. 6a). NO is one of the major effector molecules involved in the destruction of tumor cells by activated macrophages. The production of NO in vitro was assessed using the Griess reaction assay. CPS, WPS-1, WPS-2, SPS-2 and SPS-3 stimulated NO production by macrophages in a dose-dependent manner (Fig. 6b). This result is similar to the results obtained using an alkali-extractable polysaccharide (AEP) that was isolated from American ginseng roots (Yu, Yang, Cui, Wang, & Ren, 2014). In contrast, SPS-2 had no effect on NO production in the range of test doses. CPS, SPS-1 and SPS-3 had a significant effect on phagocytic activity, implying that (1 → 4)-α-D-Manp, (1 → 5)- α-L-Araf, β-D-Galp and β-D-xylose enhanced the phagocytosis of macrophages. Zha et al. (2007) stated that arabinose, mannose, xylose and galactose but not glucose played an important role in stimulating macrophage activities. Lemmon et al. (2012) provided a comprehensive model for the immunomodulatory effects of American ginseng extracts on primary human immune cells. Their results showed that a complex mixture of high molecular weight polysaccharides present in the water-soluble extracts of American ginseng accounted for most of its immunomodulatory properties. Among the five fractions obtained in this study, SPS-3 was more effective in stimulating splenic lymphocyte proliferation as well as in activating macrophages than were WPS-1, WPS-2, SPS-1 and CPS, which might be due to its high molecular weight, monosaccharide composition and complex structure. Some researchers have reported that the presence of acetyl groups and higher uronic acid content markedly affected the immunostimulatory potency of polysaccharide extracts (Lee et al., 2015; Yu et al., 2015). In this study, SPS-3 and SPS-1 were shown to contain acetyl groups using ^{1}H and ^{13}C NMR spectroscopy and were found to have a high content of uronic acid (Table 1), which might contribute to the potency of their immunostimulatory activities. Moreover, our results suggested that the polysaccharides that simultaneously exist in both α- and β-configurations (SPS-3 and SPS-1) possess higher immunostimulatory activities than do the polysaccharides (WPS-1 and WPS-2) that exist in only the α-configuration. In addition, the polysaccharide with the highest molecular weight (SPS-2, 9.7×10^{6} Da) has poor water solubility, which limited analysis of its biological activities. Based on the results of the immunomodulatory analysis and the preliminary characterization of the five fractions, it was deduced that the monosaccharide composition, uronic acid content, configuration, as well as the molecular weight, were crucial for the immunostimulatory activity of the components of the AGPS.

5. Conclusion

In summary, the present study is the first to demonstrate the purification of different polysaccharide fractions from American ginseng and to characterize some of their biological activities. The potency of their immunostimulatory effects can be ordered SPS-3 > SPS-1 > CPS > WPS-1 > WPS-2 > SPS-2. These results indicated that fraction SPS-3 has high-efficiency therapeutic immunostimulatory properties and can be utilized as an immunoadjuvant or a functional food. These findings provide a basis for further investigation of the high-efficiency and specific immunobioactive constituents of the AGPS. However, the repeating units, sugar sequence, glycosidic linkage and the degree of branching of the potent component need further research. The details on the mechanisms and structure-activity relationship would be the subject of continuing study.

Acknowledgments

This work was supported by the Application Technology Research and Development Project of China (Contract No. GC13C112) and the College Innovation Fund Project of Harbin University of Commerce (C20150008) for financial support. The authors wish to acknowledge the encouragement of Prof Ying Liu for helpful discussions regarding the preparation of the manuscript. The authors also wish to thank David Regan for providing language help.

References

Assinewe, V. A., Arnason, J. T., Aubry, A., Mullin, J., & Lemaire, I. (2002). Extractable polysaccharides of Panax quinquefolius L. (North American ginseng) root stimulate TNFα production by alveolar macrophages. *Phytomedicine*, *9*, 398–404.

Benhabiles, M. S., Drouiche, N., Lounici, H., Pauss, A., & Mameri, N. (2013). Effect of shrimp chitosan coatings as affected by chitosan extraction processes on post-harvest quality of strawberries. *Journal of Food Measurement and Characterization*, *4*, 215–221.

Chokboribal, J., Tachaboonyakiat, W., Sangvanich, P., Ruangpornvisuti, V., Jettanacheawchankit, S., & Thunyakitpisal, P. (2015). Deacetylation affects the physical properties and bioactivity of acemannan, an extracted polysaccharide from Aloe vera. *Carbohydrate Polymers*, 556–566.

Du, X. F., Jiang, C. Z., Wu, C. F., Won, E. K., & Choung, S. Y. (2008). Synergistic immunostimulating activity of pidotimod and red ginseng acidic polysaccharide against cyclophosphamide-induced immunosuppression. *Archives of Pharmacal Research*, *31*, 1153–1159.

Fang, X., Yin, X., Yuan, G., & Chen, X. (2015). Chemical and biological characterization of polysaccharides from the bark of Avicennia marina. *European Food Research and Technology*, *241*, 17–25.

Gao, H., Wang, F., Lien, E. J., & Trousdale, M. D. (1996). Immunostimulating polysaccharides from Panax notoginseng. *Pharmaceutical Research*, *8*, 1196–1200.

Hu, H., Liang, H., & Wu, Y. (2015). Isolation, purification and structural characterization of polysaccharide from Acanthopanax brachypus. *Carbohydrate Polymers*, 94–100.

Hwang, I., Ahn, G., Park, E., Ha, D., Song, J., & Jee, Y. (2011). An acidic polysaccharide of Panax ginseng ameliorates experimental autoimmune encephalomyelitis and induces regulatory T cells. *Immunology Letters*, *138*, 169–178.

Jiang, H., Sun, P., He, J., & Shao, P. (2012). Rapid purification of polysaccharides using novel radial flow ion-exchange by response surface methodology from Ganoderma lucidum. *Food and Bioproducts Processing: Transactions of the Institution of Chemical Engineers Part C*, *1*, 1–8.

Jin, M., Wang, Y., Xu, C., Lu, Z., Huang, M., & Wang, Y. (2010). Preparation and biological activities of an exopolysaccharide produced by Enterobacter cloacae Z0206. *Carbohydrate Polymers*, *3*, 607–611.

Kouakou, K., Schepetkin, I. A., Yapi, A., Kirpotina, L. N., Jutila, M. A., & Quinn, M. T. (2013). Immunomodulatory activity of polysaccharides isolated from Alchornea cordifolia. *Journal of Ethnopharmacology*, *146*, 232–242.

Lee, J., Tanikawa, T., Hayashi, K., Asagi, M., Kasahara, Y., & Hayashi, T. (2015). Characterization and biological effects of two polysaccharides isolated from Acanthopanax sciadophylloides. *Carbohydrate Polymers*, *116*, 159–166.

Lemmon, H. R., Sham, J., Chau, L. A., & Madrenas, J. J. M. M. (2012). High molecular weight polysaccharides are key immunomodulators in North American ginseng extracts: Characterization of the ginseng genetic signature in primary human immune cells. *Journal of Ethnopharmacology*, *1*, 1–13.

Li, C., Cai, J., Geng, J., Li, Y., Wang, Z., & Li, R. (2012). Purification, characterization and anticancer activity of a polysaccharide from Panax ginseng. *International Journal of Biological Macromolecules*, *51*, 968–973.

Li, Q., Xie, Y., Su, J., Ye, Q., & Jia, Z. (2012). Isolation and structural characterization of a neutral polysaccharide from the stems of Dendrobium densiflorum. *International Journal of Biological Macromolecules*, *50*, 1207–1211.

Liu, J., Luo, J., Sun, Y., Ye, H., Lu, Z., & Zeng, X. (2010). A simple method for the simultaneous decoloration and deproteinization of crude levan extract from Paenibacillus polymyxa EJS-3 by macroporous resin. *Bioresource Technology*, *15*, 6077–6083.

Ma, X. L., Hao, C. Y., Lu, S. X., Sun, Y. X., Liu, J. Z., & Liu, S. Y. (1998). Isolation and characterization of a bioactive polysaccharide from Panax quinquefolium L. *Chemical Research in Chinese Universities*, *2*, 143–146.

Maity, K., Kar Mandal, E., Maity, S., Gantait, S. K., Das, D., Maiti, S., et al. (2011). Structural characterization and study of immunoenhancing and antioxidant property of a novel polysaccharide isolated from the aqueous extract of a somatic hybrid mushroom of Pleurotus florida and Calocybe indica variety APK2. *International Journal of Biological Macromolecules*, *48*, 304–310.

Ming, Y., Qiu, T., Peng, W., Chen, W., Ye, Y., & Lin, Y. (2011). Purification, characterization and hypoglycemic activity of extracellular polysaccharides from Lachnum calyculiforme. *Carbohydrate Polymers*, *1*, 285–290.

Mondal, S., Das, D., Roy, S. K., & Islam, S. S. (2012). Isolation, purification and structural characterization of an acetylated heteroglycan from the unripe fruits of Manilkara zapota L. *Carbohydrate Research*, *354*, 74–78.

Mu, L. X., Zhu, L., Zhao, A. H., Zhou, M. M., & Jia, W. (2009). Study on extraction and purification of polysaccharides from Astragalus membranaceus. *Journal of Chinese Medicinal Materials*, *32*, 1741–1745.

Pan, D., Wang, L., Chen, C., Teng, B., Wang, C., Xu, Z., et al. (2012). Structure characterization of a novel neutral polysaccharide isolated from Ganoderma lucidum fruiting bodies. *Food Chemistry*, *135*, 1097–1103.

Prozil, S. O., Costa, E. V., Evtuguin, D. V., Cruz Lopes, L. P., & Domingues, M. R. (2012). Structural characterization of polysaccharides isolated from grape stalks of Vitis vinifera L. *Carbohydrate Research*, *356*, 252–259.

Shang, M., Zhang, X., Dong, Q., Yao, J., Liu, Q., & Ding, K. (2012). Isolation and structural characterization of the water-extractable polysaccharides from Cassia obtusifolia seeds. *Carbohydrate Polymers*, *90*, 827–832.

Sudhamani, S. R., Tharanathan, R. N., & Prasad, M. S. (2004). Isolation and characterization of an extracellular polysaccharide from Pseudomonas caryophylli CFR 1705. *Carbohydrate Polymers*, *56*, 423–427.

Sun, L., Peng, X., Sun, P., Shi, J., Yuan, X., Zhu, J., et al. (2012). Structural characterization and immunostimulatory activity of a novel linear α-(1 → 6)-D-glucan isolated from Panax ginseng C. A. Meyer. *Glycoconjugate Journal*, *29*, 357–364.

Tian, H., Yin, X., Zeng, Q., Zhu, L., & Chen, J. (2015). Isolation, structure, and surfactant properties of polysaccharides from Ulva lactuca L. from South China Sea. *International Journal of Biological Macromolecules*, *79*, 577–582.

Wang, M., Jiang, C., Ma, L., Zhang, Z., Cao, L., Liu, J., et al. (2013). Preparation, preliminary characterization and immunostimulatory activity of polysaccharide fractions from the peduncles of Hovenia dulcis. *Food Chemistry*, *138*, 41–47.

Wang, L., Yao, Y., Sang, W., Yang, X., & Ren, G. (2015). Structural features and immunostimulating effects of three acidic polysaccharides isolated from Panax quinquefolius. *International Journal of Biological Macromolecules*, *80*, 77–86.

Wang, Y., Huang, M., Sun, R., & Pan, L. (2015). Extraction, characterization of a Ginseng fruits polysaccharide and its immune modulating activities in rats with Lewis lung carcinoma. *Carbohydrate Polymers*, *127*, 215–221.

Wilson, S. A., Wong, M. H., Stryjecki, C., De Boer, A., Lui, E. M., & Mutch, D. M. (2013). Unraveling the adipocyte inflammomodulatory pathways activated by North American ginseng. *International Journal of Obesity (London)*, *37*, 350–356.

Yang, R., Meng, D., Song, Y., Li, J., Zhang, Y., Hu, X., et al. (2012). Simultaneous decoloration and deproteinization of crude polysaccharide from pumpkin residues by cross-linked polystyrene macroporous resin. *Journal of Agricultural and Food Chemistry*, *34*, 8450–8456.

Yang, W., Pei, F., Shi, Y., Zhao, L., Fang, Y., & Hu, Q. (2012). Purification, characterization and anti-proliferation activity of polysaccharides from Flammulina velutipes. *Carbohydrate Polymers*, *88*, 474–480.

Yi, Y., Zhang, M., Liao, S., Zhang, R., Deng, Y., Wei, Z., et al. (2012). Structural features and immunomodulatory activities of polysaccharides of longan pulp. *Carbohydrate Polymers*, *87*, 636–643.

Yu, Z. H., Jin, C., Xin, M., & He, J. M. (2009). Effect of Aloe vera polysaccharides on immunity and antioxidant activities in oral ulcer animal models. *Carbohydrate Polymers*, *75*, 307–311.

Yu, Z., Ming, G., Kaiping, W., Zhixiang, C., Liquan, D., Jingyu, L., et al. (2010). Structure, chain conformation and antitumor activity of a novel polysaccharide from Lentinus edodes. *Fitoterapia*, *81*, 1163–1170.

Yu, X. N., Yang, X. S., Cui, B., Wang, L. J., & Ren, G. X. (2014). Antioxidant and immunoregulatory activity of alkali-extractable polysaccharides from North American ginseng. *International Journal of Biological Macromolecules*, *42*, 357–361.

Yu, Z., Liu, L., Xu, Y., Wang, L., Teng, X., Li, X., et al. (2015). Characterization and biological activities of a novel polysaccharide isolated from raspberry (Rubus idaeus L.) fruits. *Carbohydrate Polymers*, *132*, 180–186.

Zha, X., Luo, J., Luo, S., & Jiang, S. (2007). Structure identification of a new immunostimulating polysaccharide from the stems of Dendrobium huoshanense. *Carbohydrate Polymers*, *69*, 86–93.

Zhang, S. P., Du, X. X., Zhou, Q. S., Jie, M., & Hui, L. (2011). Study on deproteinization and decoloration in fucoidan. *Advanced Materials Research*, *11*, 62–66.

Zhang, L. H., Zhao, P., Meng, Q. H., & Du, Y. P. (2014). Decolorization of limonium bicolor kunze (Bge.) polysaccharides by resins. *Advanced Materials Research*, *978*, 48–51.

Zheng, Y., Wang, W., & Li, Y. (2015). Antitumor and immunomodulatory activity of polysaccharide isolated from Trametes orientalis. *Carbohydrate Polymers*, *131*, 248–254.